Enhancing long-term memory with stimulation tunes visual attention in one trial

Robert M. G. Reinhart and Geoffrey F. Woodman[1]

Department of Psychology, Center for Integrative and Cognitive Neuroscience, Vanderbilt Vision Research Center, Vanderbilt University, Nashville, TN 37240

Edited by Michael I. Posner, University of Oregon, Eugene, OR, and approved December 1, 2014 (received for review September 6, 2014)

Scientists have long proposed that memory representations control the mechanisms of attention that focus processing on the task-relevant objects in our visual field. Modern theories specifically propose that we rely on working memory to store the object representations that provide top-down control over attentional selection. Here, we show that the tuning of perceptual attention can be sharply accelerated after 20 min of noninvasive brain stimulation over medial-frontal cortex. Contrary to prevailing theories of attention, these improvements did not appear to be caused by changes in the nature of the working memory representations of the search targets. Instead, improvements in attentional tuning were accompanied by changes in an electrophysiological signal hypothesized to index long-term memory. We found that this pattern of effects was reliably observed when we stimulated medial-frontal cortex, but when we stimulated posterior parietal cortex, we found that stimulation directly affected the perceptual processing of the search array elements, not the memory representations providing top-down control. Our findings appear to challenge dominant theories of attention by demonstrating that changes in the storage of target representations in long-term memory may underlie rapid changes in the efficiency with which humans can find targets in arrays of objects.

medial-frontal cortex | visual attention | long-term memory | executive control | transcranial direct-current stimulation

The cognitive and neural mechanisms that tune visual attention to select certain targets are not completely understood despite decades of intensive study (1, 2). Attention can clearly be tuned to certain object features (similar to tuning a radio to a specific station, also known as an attentional set), but how this tuning occurs as we search for certain objects in our environment is still a matter of debate. The prevailing theoretical view is that working memory representations of target objects provide top-down control of attention as we perform visual search for these objects embedded in arrays of distractors (3–7). However, an alternative view is that long-term memory representations play a critical role in the top-down control of attention, enabling us to guide attention based on the more enduring representations of this memory store (8–16). To distinguish between these competing theoretical perspectives, we used transcranial direct-current stimulation (tDCS) to manipulate activity in the brain causally (17), and combined this causal manipulation of neural activity with electrophysiological measurements that are hypothesized to index the working memory and long-term memory representations that guide visual attention to task-relevant target objects.

To determine the nature of the working memory and long-term memory representations that control visual attention during search, we simultaneously measured two separate human event-related potentials (ERPs) (8, 18, 19). The contralateral delay activity (or CDA) of subjects' ERPs provides a measure of the maintenance of target object representations in visual working memory (20, 21). The CDA is a large negative waveform that is maximal over posterior cortex, contralateral to the position of a remembered item. This large-amplitude lateralized negativity is observed even when nonspatial features are being remembered, and persists as information is held in working memory to perform a task. A separate component, termed the anterior P1, or P170, is hypothesized to measure the build-up of long-term memory representations. The anterior P1 is a positive waveform that is maximal over frontal cortex and becomes increasingly negative as exposures to a stimulus accumulate traces in long-term memory (8, 19, 22). This component is thought to reflect the accumulation of information that supports successful recognition of a stimulus on the basis of familiarity (23). For example, the anterior P1 amplitude can be used to predict subsequent recognition memory for a stimulus observed hundreds of stimuli in the past (i.e., across minutes to hours of time) (23) (additional information on the critical features of these ERP components is provided in *SI Materials and Methods*). We used simultaneous measurements of the CDA and anterior P1 to determine the role that working memory and long-term memory representations play in the tuning of attention following brain stimulation.

Our tDCS targeted the medial-frontal region in our first experiments (Fig. 1*A*) because anodal stimulation of this area results in rapid improvement of simple visual discriminations relative to baseline sham conditions (24). If it is possible to induce rapid improvements in the selection of targets among distractors as humans perform search, then the competing theories of visual attention would account for the accelerated tuning of attention in different ways. The theories that propose working memory representations provide top-down control of visual attention predict that the stimulation-induced improvement in visual search will be due to changes in the nature of the visual working memory representations indexed by the CDA component (Fig. 1 *B* and *C*). Specifically, the CDA elicited by the target cue presented on each trial should increase in amplitude, relative to the sham condition, to explain the improvement of attentional selection during search. This type of modulation is expected if

Significance

Theories of attention propose that we rely on working memory to control attention by maintaining target presentations in this active store as our visual systems are used to search for certain objects. Here, we show that the tuning of perceptual attention can be sharply accelerated by noninvasive brain stimulation. Our electrophysiological measurements showed that these improvements in attentional tuning were preceded by changes in event-related potentials thought to index long-term memory, but not those potentials that index working memory. Our findings support the hypothesis that changes in the storage of target representations in long-term memory may underlie rapid changes in how target objects are selected by visual attention.

Author contributions: R.M.G.R. and G.F.W. designed research; R.M.G.R. performed research; R.M.G.R. analyzed data; and R.M.G.R. and G.F.W. wrote the paper.

The authors declare no conflict of interest.

This article is a PNAS Direct Submission.

[1]To whom correspondence should be addressed. Email: geoffrey.f.woodman@vanderbilt.edu.

This article contains supporting information online at www.pnas.org/lookup/suppl/doi:10.1073/pnas.1417259112/-/DCSupplemental.

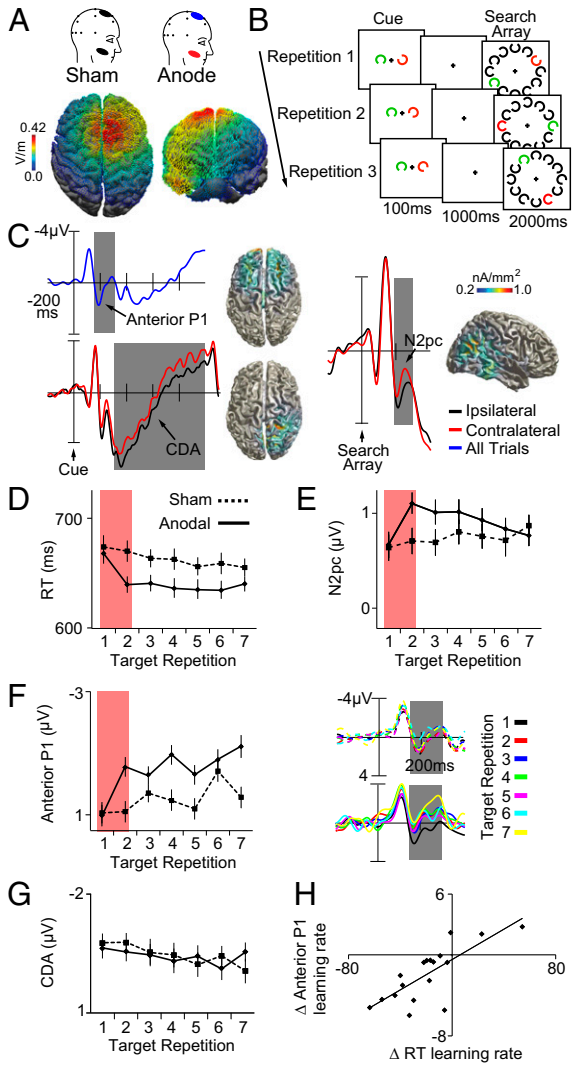

Fig. 1. tDCS model, task, and results of experiment 1. (*A*) Modeled distribution of current during frontocentral midline anodal tDCS on top and front views of a 3D reconstruction of the cortical surface. (*B*) Task-relevant cue (green Landolt C in this example) signaled the shape of the target in the upcoming search array. Subjects searched for the same target across a run of three to seven trials. Central fixation was maintained for the trial duration. (*C*) Representative anterior P1, CDA, and N2pc from repetition 1 in the sham condition show each component's distinctive temporal and spatial profile, with analysis windows shaded in gray. Mean RTs (*D*), N2pc amplitudes (*E*), anterior P1 amplitudes (*F*), and CDA amplitudes (*G*) are shown across target repetitions for sham (dashed line) and anodal (solid line) conditions. Error bars are ±1 SEM. Red shading highlights dynamics across trials 1 and 2. Grand average ERP waveforms from the frontal midline electrode (Fz) synchronized to cue onset are shown across target repetitions for sham (dashed line) and anodal (solid line) conditions. The measurement window of the anterior P1 is shaded in gray. (*H*) Relationship between logarithmic rate parameter enhancements for mean anterior P1 amplitude and RT after anodal stimulation relative to sham.

working memory-driven theories of attention are correct based on previous evidence that the CDA is larger on trials of a short-term memory task when performed correctly compared with incorrect trials (20). In contrast, theories that propose long-term memory representations rapidly assume control of attention during visual search predict that the stimulation-induced improvement will be due to changes in the long-term memory representations indexed by the anterior P1 elicited by the target cue presented on each trial. Specifically, we should see the anterior P1 exhibit a more negative potential as search improves following stimulation.

Each subject completed anodal and sham tDCS sessions on different days, with order counterbalanced across subjects ($n = 18$). Immediately after 20 min of tDCS over medial-frontal (experiments 1 and 2) or right parietal (experiment 3) regions of the head (see the current flow model for experiment 1 in Fig. 1*A*, and additional information about stimulation locations in *SI Materials and Methods*), we recorded subjects' ERPs while they completed a visual search task. In this search task, the target was cued at the beginning of each trial (Fig. 1 *B* and *C*). The task-relevant cue signaled the identity of the target that could appear in the search array presented a second later. In experiments 1 and 3, the targets and distractors were Landolt-C stimuli, and in experiment 2, they were pictures of real-world objects. A task-irrelevant item was presented with each cue to balance the hemispheric visual input so that the lateralized ERPs that elicit the CDA could be unambiguously interpreted (25). The key manipulation in this task was that the target remained the same for three to seven consecutive trials (length of run randomized) before it was changed to a different object. These target repetitions allowed us to observe attentional tuning becoming more precise across trials.

We found that anodal medial-frontal tDCS in experiment 1 accelerated the rate of attentional tuning across trials, as evidenced by the speed of behavior and attention-indexing ERPs elicited by the search arrays (Fig. 1 *D* and *E*). First, in the baseline sham condition, we observed that subjects became faster at searching for the target across the same-target runs of trials, as shown by reaction time (RT) speeding ($F_{2,34} = 6.031$, $P = 0.007$) (additional analyses of the sham condition and analyses to verify the absence of effects on accuracy are provided in Fig. S1*A* and *SI Materials and Methods*). However, following anodal stimulation, subjects' RTs dramatically increased in speed, such that search RTs reached floor levels within a single trial. This striking causal aftereffect of anodal tDCS was evidenced by a stimulation condition × target repetition interaction on RTs ($F_{2,34} = 3.735$, $P = 0.042$), with this RT effect being significant between the first two trials of search for a particular Landolt C ($F_{1,17} = 6.204$, $P = 0.023$) but with no significant change thereafter ($P > 0.310$). Additionally, by fitting these behavioral RT data with a logarithmic function to model the rate of improvement (9), we found that anodal tDCS significantly increased the rate parameters of RT speeding ($F_{1,17} = 5.097$, $P = 0.037$).

Consistent with the interpretation that tDCS changed how attention selected the targets in the search arrays, we found that the N2-posterior-contralateral (N2pc) component, an index of the deployment of covert attention to the possible target in a search array (26), showed a pattern that mirrored the single-trial RT effects ($F_{1,17} = 4.792$, $P = 0.043$) (Fig. 1*E*; N2pc waveforms are provided in Fig. S1*A*). However, other ERP components indexing lower level perceptual processing or late-stage response selection during search were unchanged by the tDCS (Fig. S1 *C* and *D* and Table S1). Our findings demonstrate that the brain stimulation only changed the deployment of visual attention to targets in the search arrays and did not change the operation of any other cognitive mechanism we could measure during the visual search task. Thus, by delivering electrical current over the medial-frontal area, we were able to accelerate the speed with which subjects tuned their attention to select the task-relevant objects causally.

To determine whether the tDCS-induced attentional improvements were caused by changes in working memory or long-term memory mechanisms of top-down control, we examined the putative neurophysiological signatures of visual working memory (i.e., the CDA) and long-term memory (i.e., the anterior P1) elicited by the target cues. Given the rapid tuning of attention following tDCS relative to sham, we might expect the flexible working memory system to underlie this effect. Contrary to this intuition, we found that the rapid, one-trial improvement in

attentional tuning following medial-frontal tDCS was mirrored by changes in the putative neural index of long-term memory but left the putative neural index of working memory unchanged (Fig. 1 *F* and *G*). Fig. 1*F* shows that the accelerated effects of attentional tuning caused by anodal stimulation were preceded by a rapid increase in negativity of the anterior P1 across same-target trials, mirroring the rapid, single-trial improvement in RT and the N2pc as the search array was analyzed. This effect was confirmed statistically by a significant stimulation condition × target repetition interaction on the anterior P1 amplitude ($F_{2,34} = 3.797$, $P = 0.049$), and most dramatically between the first two trials of search ($F_{1,17} = 5.816$, $P = 0.027$), with no significant pairwise changes in anterior P1 amplitude thereafter ($P > 0.707$). Logarithmic model fits showed that the rate parameters of the anterior P1 significantly increased after anodal tDCS relative to the more gradual attentional tuning observed in the sham condition ($F_{1,17} = 5.502$, $P = 0.031$; anterior P1 analyses from the sham condition are described in *SI Materials and Methods*). Despite these causal changes in anterior P1 activity, neither the amplitude of the CDA ($F_{2,34} = 0.669$, $P = 0.437$) nor its rate parameters ($F_{1,17} = 1.183$, $P = 0.292$) significantly differed between stimulation conditions, showing the selectivity of medial-frontal tDCS on the putative neural metric of long-term memory (CDA waveforms are provided in Fig. S1*B*). We note that the absence of a stimulation-induced CDA increase is not due to ceiling effects. The single target cue gave us ample room to measure such a boost of the CDA, given that without brain stimulation, this memory load is far from eliciting ceiling amplitude levels for this component (20).

If the better long-term memory representations indexed by the anterior P1 were the source of the improved search performance, then the size of the stimulation-induced boost of the anterior P1 elicited by the cue should be predictive of the search performance that followed a second later. Consistent with the prediction, we found that an individual subject's anterior P1 amplitude change across the same-target runs following medial-frontal stimulation was highly predictive of the accelerated rates at which the subjects searched through the visual search array that followed ($r_{18} = 0.764$, $P = 0.0002$) (Fig. 1*H*). Thus, the ERPs elicited by the target cues ruled out the working memory explanation of the rapid changes in attentional tuning we observed, and were consistent with the hypothesis that changes in the nature of the long-term memory representations that control attention were the source of this dramatic improvement.

In experiment 2, we replicated the pattern of findings from experiment 1 using a search task in which the targets and distractors were pictures of real-world objects (Fig. 2 and Fig. S2). These results demonstrate the robustness and reliability of the pattern of effects shown in experiment 1. Specifically, brain stimulation resulted in attention being rapidly retuned to the new targets after one trial, as evidenced by RTs hitting the floor by the second trial in a run. Again, this change in RT was mirrored by stimulation changing the anterior P1, and not the CDA, consistent with accounts that posit an important role for long-term memory in the guidance of attention.

Next, we sought to provide converging evidence for our conclusion that the stimulation was changing subjects' behavior by changing the nature of subjects' long-term memory, consistent with previous functional interpretations of the anterior P1. So far, we have drawn conclusions using our analyses across the fairly short runs of same-target trials. However, we next looked at the learning that took place across the entire experimental session, lasting almost 3 h. If our interpretation of the anterior P1 underlying accelerated attentional tuning is correct, then we should see that the anterior P1 is sensitive to the accumulative effects of learning across the entire experimental session and that these long-term effects change following stimulation. To assess the cumulative effects of learning across these long experimental sessions, we examined how behavior, the anterior P1,

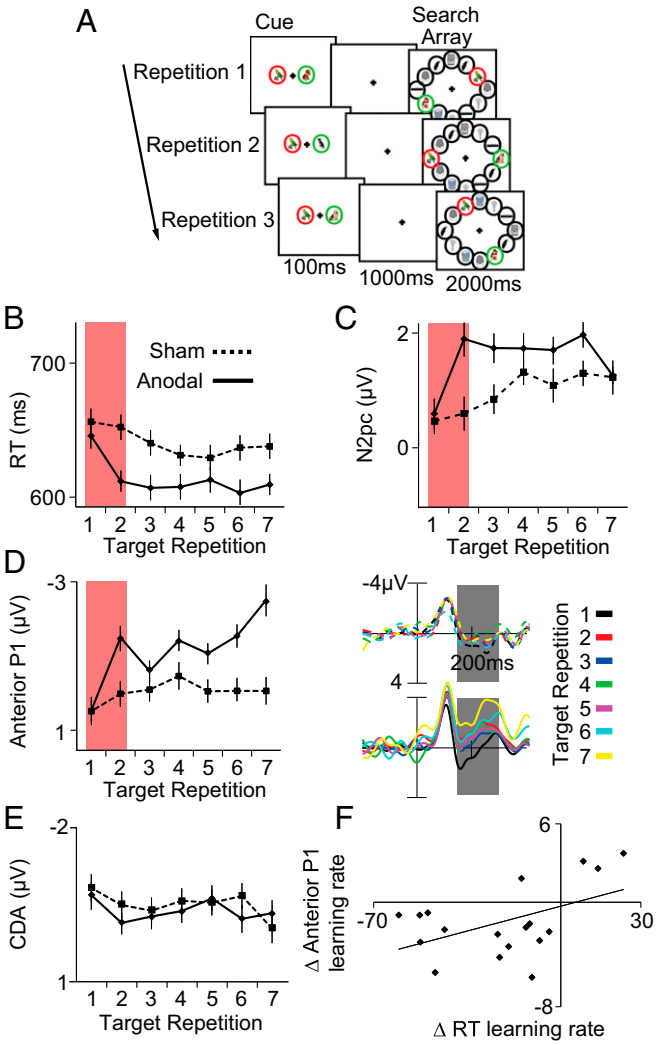

Fig. 2. Task and results of experiment 2. (*A*) Task in experiment 2 was identical to that of experiment 1 with the exception that Landolt-C stimuli were replaced with real-world objects. Mean RTs (*B*), N2pc amplitudes (*C*), anterior P1 amplitudes (*D*), and CDA amplitudes (*E*) are shown across target repetitions for sham (dashed line) and anodal (solid line) conditions. Error bars are ±1 SEM. Red shading highlights dynamics across trials 1 and 2. Grand average ERP waveforms from the frontal midline electrode (Fz) synchronized to cue onset are shown across target repetitions for sham (dashed line) and anodal (solid line) conditions. The measurement window of the anterior P1 is shaded in gray. (*F*) Relationship between logarithmic rate parameter enhancements for mean anterior P1 amplitude and RT after anodal stimulation relative to sham.

and the CDA changed across the beginning, middle, and end of experiments 1 and 2 (Fig. 3 and *SI Materials and Methods*); that is, we averaged the same-target runs together in the first third, second third, and final third of sessions across all of our subjects. Fig. 3 shows the learning we observed across these long sessions. The RTs were slowest at the beginning of the experiment, when faced with a new target, but as subjects accumulated experience with the set of eight possible targets, we saw the RTs at the beginning of the same-target runs become progressively faster. This accumulation of experience across the entire session that sped RT was mirrored by systematic changes in the amplitude of the anterior P1. The anterior P1 became progressively more negative across the experiment, as we would expect if the magnitude of the negativity were indexing the quality (i.e., strength or number) of the long-term memories for these targets that

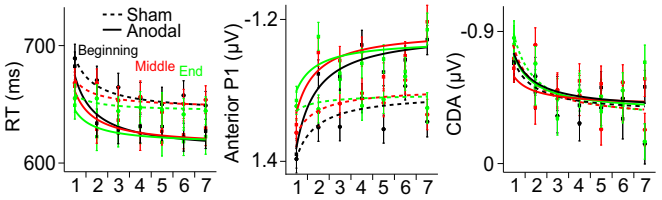

Fig. 3. Within-session dynamics of experiments 1 and 2. Mean RT, anterior P1 amplitude, and CDA amplitude as a function of target repetitions binned according to the first third (black), middle third (red), and last third (green) of runs, collapsed across experiments 1 and 2. Logarithmic model fits are shown for sham (dashed line) and anodal (solid line) tDCS conditions. Error bars are ±1 SEM.

accumulated across the entire experiment. In contrast, the CDA showed no change across the entire experiment, indicating that the role of working memory in updating the target at the beginning of the same-target runs does not change with protracted learning. For example, it is likely that working memory representations were reactivated to help reduce proactive interference from the target representations built up during the previous run of trials, consistent with influential theoretical proposals (27). Our medial-frontal tDCS boosted these learning effects measured with the anterior P1 and search RTs while leaving the CDA unchanged, consistent with our interpretation of the findings across the shorter same-target runs. Thus, this cumulative learning across the entire experimental session allowed us to observe how the dynamics of the memory representations underlying the focusing of attention evolved over the long term. These results lend further support to the hypothesis that contributions from long-term memory are driving the causal boost of attentional tuning we observed following brain stimulation.

To determine whether the effects of experiments 1 and 2 were specific to medial-frontal stimulation, in experiment 3, we stimulated the posterior parietal region in a new group of subjects (order of anodal and sham conditions was counterbalanced, $n = 18$) (Fig. 4*A*). This region of the dorsal visual stream plays a role in memory (28) and generating top-down attentional control signals (29), so that it provides a useful contrast with our medial-frontal stimulation, which appeared to influence attentional selection by changing the long-term memory representations. We specifically targeted the right parietal region because previous studies show that disrupting activity in right parietal cortex can influence attention (30, 31).

We found that unlike medial-frontal stimulation, right parietal tDCS had no effect on the overall tuning of attention or the memory representations controlling search performance. Fig. 4 *B–E* shows the overlap between stimulation conditions for the RTs (no stimulation condition × target repetition interaction: $F_{2,34} = 0.029$, $P = 0.955$) and the amplitudes of the N2pc ($F_{2,34} = 0.139$, $P = 0.807$), CDA ($F_{2,34} = 0.814$, $P = 0.439$), and anterior P1 ($F_{2,34} = 0.393$, $P = 0.663$) across target repetitions. Because subjects again searched for the same target across the runs of trials in experiment 3, we did observe main effects of target repetition on RTs ($F_{2,34} = 6.190$, $P = 0.015$) and the amplitudes of the N2pc ($F_{2,34} = 4.053$, $P = 0.045$), CDA ($F_{2,34} = 5.292$, $P = 0.024$) and anterior P1 ($F_{2,34} = 6.320$, $P = 0.006$). These effects were due to the steady speeding of RTs, declining CDA amplitude, and increasing amplitudes of the anterior P1 and N2pc across same-target trials. The effects of target repetition indicate that the roles played by working memory and long-term memory in tuning attention across

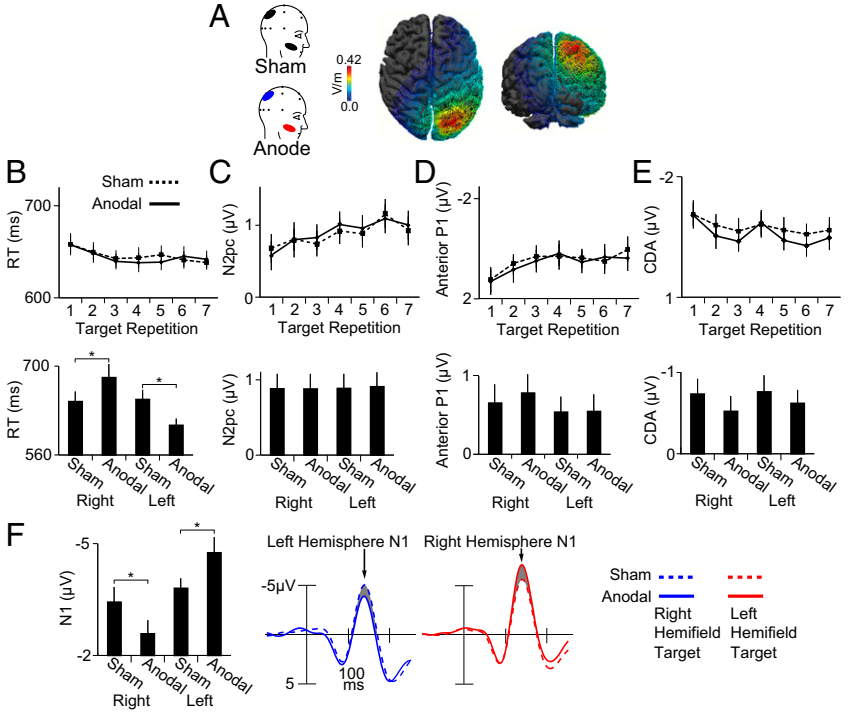

Fig. 4. tDCS model and results of experiment 3. (*A*) Modeled distribution of current during right parietal anodal tDCS on top and rear views of a 3D reconstruction of the cortical surface. Mean RTs (*B*), N2pc amplitudes (*C*), anterior P1 amplitudes (*D*), and CDA amplitudes (*E*) are shown across target repetitions for sham (dashed line) and anodal (solid line) conditions. Bar graphs show data collapsed across target repetitions for each stimulation condition based on whether the target color appeared in the left or right visual hemifield. Error bars are ±1 SEM. (*F*) Mean N1 amplitudes are illustrated as in *B–E*. The waveforms are search array-locked grand average potentials at lateral occipital sites (OL/OR) contralateral to right (blue) and left (red) hemifield target colors shown across sham (dashed line) and anodal (solid line) conditions. OL, occipital left; OR, occipital right. *$P < 0.05$.

trials in the baseline sham condition were unchanged following right parietal stimulation (Fig. 4 *B–E* and Figs. S3*D* and S4).

Given the lateralized application of tDCS in experiment 3, we examined the data based on whether the target appeared in the left or right visual field. We found that parietal stimulation caused lateralized, bidirectional effects on search performance. Relative to sham, subjects were faster at searching for targets after anodal stimulation, but only on trials in which the target color appeared contralateral (i.e., in the left visual field) to the location of the stimulating electrode on the head (i.e., over the right hemisphere) (Fig. 4*B*). This effect was evidenced by a stimulation condition × target color laterality interaction on search RTs ($F_{1,17} = 12.098$ $P = 0.003$) and a main effect of stimulation condition on contralateral search RTs ($F_{1,17} = 6.014$ $P = 0.025$). In contrast, RTs were slower when target colors appeared ipsilateral (i.e., in the right visual hemifield) with respect to the location of tDCS ($F_{1,17} = 4.276$ $P = 0.054$) (Fig. 4*B*). These results suggest that parietal stimulation facilitated and impeded overall search behavior depending on the location of the target in the visual field.

We found that the lateralized, bidirectional effects of parietal tDCS on search performance were caused by directly influencing perceptual processing, not changing the memory representations controlling attention. The amplitude of the posterior N1 component, a neural index of perceptual processing (32), was significantly modulated by stimulation condition and in a pattern mirroring that of the behavior (stimulation condition × target color laterality interaction: $F_{1,17} = 10.494$ $P = 0.005$; stimulation condition main effects: contralateral, $F_{1,17} = 4.755$ $P = 0.044$; stimulation condition main effects: ipsilateral, $F_{1,17} = 4.573$ $P = 0.047$) (Fig. 4*F* and Fig. S3*A*). In contrast, our indices of the memory representations of the targets and of the deployment of attention were not significantly changed by tDCS [i.e., no stimulation condition × target color laterality interaction: N2pc ($F_{1,17} = 0.041$ $P = 0.843$), CDA ($F_{1,17} = 0.107$ $P = 0.748$), anterior P1 ($F_{1,17} = 0.169$ $P = 0.686$)] (Fig. 4 *C–E* and Fig. S3 *B–D*).

In sum, our parietal stimulation protocol did not change the nature of the memory representations controlling attention but directly influenced the perceptual processing of the objects in the search array. These observations were evidenced by lateralized changes in the early visual ERPs and the behavioral responses to the task-relevant items contralateral vs. ipsilateral to the stimulation. Thus, the effects observed in experiments 1 and 2 are not a ubiquitous pattern observed following stimulation of any cognitive control structure. Instead, when we stimulated the posterior parietal region of the visual stream, we observed changes in early visual responses of the brain and similarly spatially mapped patterns of performance.

Our findings from experiments 1 and 2, that stimulation over medial-frontal areas can rapidly improve attentional selection of targets, may seem surprising because the medial-frontal cortex is not commonly thought to be a crucial node in the network of regions that guide attention (29, 33). This region is most frequently discussed as critical for the higher level monitoring of task performance, response conflict, and prediction error (34, 35). However, a variety of studies across species and methods have found connections between regions of medial-frontal cortex and both attention and memory processes. First, human neuroimaging research shows that the cingulate opercular network, including anterior cingulate and presupplementary cortex, is engaged during the implementation of a task set, visuospatial attention, and episodic memory (36–38). Second, studies using animal models show that attentional selectivity in the visual domain appears to reside in dorsomedial areas of prefrontal cortex (39), such as the anterior cingulate gyrus. Third, both the dorsomedial and right dorsolateral prefrontal cortices respond strongly in memory recognition tasks with specific activity bordering the anterior cingulate at or near Brodmann's areas 6, 8, and 32 (40), including supplementary and presupplementary motor areas. The right dorsolateral prefrontal cortex, which also appeared to be in the path of our current-flow modeling, has been causally linked to human long-term memory processes (41). Given the set of regions in this path, the specificity of our empirical observations is striking. However, future work is clearly needed to dissect the contributions of the group of medial-frontal and medial-prefrontal regions within the path of the current used here.

Our results present evidence from causal manipulations of the healthy human brain that suggest the rapid reconfiguration of the top-down control of visual attention can be carried out by long-term memory. This conclusion seems counterintuitive, given that the active storage of objects in working memory can strongly control attention (7, 18, 42) and that the dominant theories of attention focus exclusively on the role of working memory in guiding attention (3–6). The present findings do not suggest that working memory representations do not control attention across the short term; indeed, we observed the neural index of storage of the target in working memory that was concurrent with the large changes in the putative index of long-term memory. The critical implication of the present findings is that the rapid improvements in attentional control following brain stimulation were most closely related to our ERP measure of long-term memory and not working memory. These results are surprising to us, given that effects of long-term memory on attentional control are typically observed in tasks in which improvements evolve slowly across protracted training (10, 12–14, 16, 43), or even a lifetime of semantic associations (11). Here, we show that the time course of improvement need not be diagnostic of the type of memory representation involved.

Our results can also be interpreted within theoretical models that take a broader view of top-down control and do not rely on a conceptual dichotomy between working memory and long-term memory processes that guide attention (44). Neuroimaging research has identified multiple control mechanisms that configure downstream processing consistent with behavioral goals. Most relevant here is the network consisting of the anterior insula (also referred to as the frontal operculum) and dorsal anterior cingulate cortex (also referred to as the medial superior frontal cortex). This network is thought to integrate information over protracted time scales, in an iterative manner, similar to the dynamics and functional properties of the anterior P1. Further, the cingulate opercular network carries various critical control signals, including the selection and maintenance of task goals and the making and monitoring of choices (38, 45, 46). It is possible that our medial-frontal stimulation changed the functioning of this control network, causing the improvements we observed in attentional control.

Finally, our findings provide evidence from causal manipulations of the human brain to support the slowly growing view that the nature of top-down attentional control involves the interplay of different types of memory representations (8, 15, 47–49). Moving forward, we believe that such a view moves theories of attention nearly into register with models of learning, automaticity, and skill acquisition (9, 50–52). Ideally, this perspective will serve to unify, rather than further hyperspecialize, theories of information processing in the brain.

Materials and Methods

Subjects. Eighteen subjects participated in each experiment (additional subject information is provided in *SI Materials and Methods*). All had normal color vision and normal or corrected-to-normal visual acuity, and gave informed consent to participate in the study approved by the Vanderbilt University Institutional Review Board.

tDCS. The tDCS was administered using a battery-driven, constant-current stimulator (Mind Alive, Inc.) through a pair of conductive rubber electrodes (active, 19.25 cm^2; reference, 52 cm^2). The electrodes were placed in

saline-soaked synthetic sponges and held in place by a headband. The reference (or cathodal) electrode was placed on the center of the right cheek (Fig. 1*A*).

Current was applied at 2.0 mA for 20 min over the medial-frontal region (site FCz, from the International 10–20 System) for experiments 1 and 2, and over the right parietal region (site P2) for experiment 3. A sham tDCS condition was administered using an identical procedure, but stimulation only lasted 30 s, ramping up and down at the beginning, middle, and end of the 20-min period to simulate the periodic tingling sensation often endorsed by subjects on active stimulation days. Debriefing questions confirmed that subjects were blinded, and could not distinguish between sham and anodal stimulation.

Stimuli and Task. Following the active or sham stimulation, subjects performed a cued visual search task while their EEG was recorded so that we could extract their ERPs using our standard methods (18, 19) (additional details are provided in *SI Materials and Methods*). Each trial of the task began with fixation (1,200–1,600 ms). Next, two cue stimuli were presented for 100 ms, followed by a 1,000-ms interval during which we measured the CDA and anterior P1. Then, the search array was presented for 2,000 ms (additional metrics describing these stimuli are provided in *SI Materials and Methods*). The intertrial interval was 1,200–1,600 ms, randomly jittered with a rectangular distribution.

In all experiments, a target matched the shape of the Landolt C (experiments 1 and 3) or picture (experiment 2) of the task-relevant cue. Every search array contained an item that matched the color of the cue object (i.e., the possible target), but on target absent trials, this object had a different shape (half of trials). Subjects responded as quickly and accurately as possible to the search array by pressing one button on a handheld gamepad with their right hand for target present and a different button with their right hand for target absent. The task-relevant color in experiments 1 and 3 (i.e., red or green) and the task-relevant real-world object category in experiment 2 (i.e., dog or bird) were counterbalanced across subjects to rule out physical stimulus confounds.

Target presence and possible target location were randomly selected on each trial. The same target was cued across a run of three, five, or seven trials, randomly varying in length, with the identity of the target randomly selected for each run without repetition in adjacent runs. Each subject completed 720 trials in each condition (sham and anodal).

Additional details about the methods used in this study are provided in *SI Materials and Methods*.

ACKNOWLEDGMENTS. We thank Laura McClenahan for help with data collection. This work was supported by Grants R01-EY019882, P30-EY08126, F31-MH102042, and T32-EY007135 from the NIH and Grant BCS-0957072 from the National Science Foundation.

1. Wolfe JM, Horowitz TS (2004) What attributes guide the deployment of visual attention and how do they do it? *Nat Rev Neurosci* 5(6):495–501.
2. Gilbert CD, Li W (2013) Top-down influences on visual processing. *Nat Rev Neurosci* 14(5):350–363.
3. Bundesen C (1990) A theory of visual attention. *Psychol Rev* 97(4):523–547.
4. Bundesen C, Habekost T, Kyllingsbaek S (2005) A neural theory of visual attention: Bridging cognition and neurophysiology. *Psychol Rev* 112(2):291–328.
5. Desimone R, Duncan J (1995) Neural mechanisms of selective visual attention. *Annu Rev Neurosci* 18:193–222.
6. Duncan J, Humphreys GW (1989) Visual search and stimulus similarity. *Psychol Rev* 96(3):433–458.
7. Olivers CNL, Peters J, Houtkamp R, Roelfsema PR (2011) Different states in visual working memory: When it guides attention and when it does not. *Trends Cogn Sci* 15(7):327–334.
8. Woodman GF, Carlisle NB, Reinhart RMG (2013) Where do we store the memory representations that guide attention? *J Vis* 13(3):1–7.
9. Logan GD (2002) An instance theory of attention and memory. *Psychol Rev* 109(2): 376–400.
10. Wolfe JM (2012) Saved by a log: How do humans perform hybrid visual and memory search? *Psychol Sci* 23(7):698–703.
11. Moores E, Laiti L, Chelazzi L (2003) Associative knowledge controls deployment of visual selective attention. *Nat Neurosci* 6(2):182–189.
12. Chun MM (2000) Contextual cueing of visual attention. *Trends Cogn Sci* 4(5):170–178.
13. Summerfield JJ, Lepsien J, Gitelman DR, Mesulam MM, Nobre AC (2006) Orienting attention based on long-term memory experience. *Neuron* 49(6):905–916.
14. Stokes MG, Atherton K, Patai EZ, Nobre AC (2012) Long-term memory prepares neural activity for perception. *Proc Natl Acad Sci USA* 109(6):E360–E367.
15. Hutchinson JB, Turk-Browne NB (2012) Memory-guided attention: Control from multiple memory systems. *Trends Cogn Sci* 16(12):576–579.
16. Võ ML-H, Wolfe JM (2012) When does repeated search in scenes involve memory? Looking at versus looking for objects in scenes. *J Exp Psychol Hum Percept Perform* 38(1):23–41.
17. Nitsche MA, et al. (2008) Transcranial direct current stimulation: State of the art 2008. *Brain Stimulat* 1(3):206–223.
18. Carlisle NB, Arita JT, Pardo D, Woodman GF (2011) Attentional templates in visual working memory. *J Neurosci* 31(25):9315–9322.
19. Reinhart RMG, Woodman GF (2014) High stakes trigger the use of multiple memories to enhance the control of attention. *Cereb Cortex* 24(8):2022–2035.
20. Vogel EK, Machizawa MG (2004) Neural activity predicts individual differences in visual working memory capacity. *Nature* 428(6984):748–751.
21. Vogel EK, McCollough AW, Machizawa MG (2005) Neural measures reveal individual differences in controlling access to working memory. *Nature* 438(7067):500–503.
22. Voss JL, Schendan HE, Paller KA (2010) Finding meaning in novel geometric shapes influences electrophysiological correlates of repetition and dissociates perceptual and conceptual priming. *Neuroimage* 49(3):2879–2889.
23. Tsivilis D, Otten LJ, Rugg MD (2001) Context effects on the neural correlates of recognition memory: An electrophysiological study. *Neuron* 31(3):497–505.
24. Reinhart RMG, Woodman GF (2014) Causal control of medial-frontal cortex governs electrophysiological and behavioral indices of performance monitoring and learning. *J Neurosci* 34(12):4214–4227.
25. Woodman GF (2010) A brief introduction to the use of event-related potentials in studies of perception and attention. *Atten Percept Psychophys* 72(8):2031–2046.
26. Woodman GF, Luck SJ (1999) Electrophysiological measurement of rapid shifts of attention during visual search. *Nature* 400(6747):867–869.
27. Kane MJ, Engle RW (2002) The role of prefrontal cortex in working-memory capacity, executive attention, and general fluid intelligence: An individual-differences perspective. *Psychon Bull Rev* 9(4):637–671.
28. Eichenbaum H, Cohen NJ (2001) *From Conditioning to Conscious Recollection: Memory Systems of the Brain* (Oxford Univ Press, Oxford).
29. Corbetta M, Shulman GL (2002) Control of goal-directed and stimulus-driven attention in the brain. *Nat Rev Neurosci* 3(3):201–215.
30. Beck DM, Muggleton N, Walsh V, Lavie N (2006) Right parietal cortex plays a critical role in change blindness. *Cereb Cortex* 16(5):712–717.
31. Tseng P, et al. (2010) Posterior parietal cortex mediates encoding and maintenance processes in change blindness. *Neuropsychologia* 48(4):1063–1070.
32. Luck SJ, Hillyard SA (1990) Electrophysiological evidence for parallel and serial processing during visual search. *Percept Psychophys* 48(6):603–617.
33. Buschman TJ, Miller EK (2007) Top-down versus bottom-up control of attention in the prefrontal and posterior parietal cortices. *Science* 315(5820):1860–1862.
34. Brown JW, Braver TS (2005) Learned predictions of error likelihood in the anterior cingulate cortex. *Science* 307(5712):1118–1121.
35. Shenhav A, Botvinick MM, Cohen JD (2013) The expected value of control: An integrative theory of anterior cingulate cortex function. *Neuron* 79(2):217–240.
36. Sestieri C, Corbetta M, Spadone S, Romani GL, Shulman GL (2014) Domain-general signals in the cingulo-opercular network for visuospatial attention and episodic memory. *J Cogn Neurosci* 26(3):551–568.
37. Dosenbach NUF, et al. (2007) Distinct brain networks for adaptive and stable task control in humans. *Proc Natl Acad Sci USA* 104(26):11073–11078.
38. Dosenbach NU, et al. (2006) A core system for the implementation of task sets. *Neuron* 50(5):799–812.
39. Dalley JW, Cardinal RN, Robbins TW (2004) Prefrontal executive and cognitive functions in rodents: Neural and neurochemical substrates. *Neurosci Biobehav Rev* 28(7): 771–784.
40. Wagner AD, Desmond JE, Glover GH, Gabrieli JD (1998) Prefrontal cortex and recognition memory. Functional-MRI evidence for context-dependent retrieval processes. *Brain* 121(Pt 10):1985–2002.
41. Rossi S, et al. (2001) Prefrontal [correction of Prefontal] cortex in long-term memory: An "interference" approach using magnetic stimulation. *Nat Neurosci* 4(9):948–952.
42. Chelazzi L, Miller EK, Duncan J, Desimone R (1993) A neural basis for visual search in inferior temporal cortex. *Nature* 363(6427):345–347.
43. Chun MM, Jiang Y (1998) Contextual cueing: Implicit learning and memory of visual context guides spatial attention. *Cognit Psychol* 36(1):28–71.
44. Dosenbach NU, Fair DA, Cohen AL, Schlaggar BL, Petersen SE (2008) A dual-networks architecture of top-down control. *Trends Cogn Sci* 12(3):99–105.
45. Johnston K, Levin HM, Koval MJ, Everling S (2007) Top-down control-signal dynamics in anterior cingulate and prefrontal cortex neurons following task switching. *Neuron* 53(3):453–462.
46. Rushworth MF, Buckley MJ, Behrens TE, Walton ME, Bannerman DM (2007) Functional organization of the medial frontal cortex. *Curr Opin Neurobiol* 17(2):220–227.
47. Woodman GF, Chun MM (2006) The role of working memory and long-term memory in visual search. *Vis Cogn* 14(4-8):808–830.
48. Pillsbury WB (1908) *Attention* (Macmillan, New York).
49. Chun MM, Turk-Browne NB (2007) Interactions between attention and memory. *Curr Opin Neurobiol* 17(2):177–184.
50. Rickard TC (1997) Bending the power law: A CMPL theory of strategy shifts and the automatization of cognitive skills. *J Exp Psychol Gen* 126(3):288–311.
51. Anderson JR (1982) Acquisition of a cognitive skill. *Psychol Rev* 89(4):369–406.
52. Anderson JR (2000) *Learning and Memory* (Wiley, New York).

Supporting Information

Reinhart and Woodman 10.1073/pnas.1417259112

SI Materials and Methods

Background. Our methodological approach in the present study took advantage of a set of independent ERP tools that have been established to track the target templates represented in visual working memory and long-term memory simultaneously. This section provides a brief summary of the evidence on which the present study is built, demonstrating the logic behind using these tools to understand the nature of the memory representations that control attention.

CDA as an index of visual working memory. In the present study, it was possible to track the representation of targets in visual working memory using the CDA of subjects' ERP waveforms. Previous ERP research has demonstrated that when subjects are holding representations of objects in visual working memory, a sustained negative potential is found over the hemisphere contralateral to the position of the objects in the visual field. This memory-related ERP component exploits the lateralization of the visual system and, as a result, is known as the CDA (1–3). This work shows that the CDA provides a measure of the objects represented in working memory, increasing in amplitude up to each individual's visual working memory capacity, provided the objects are task-relevant and happen to be lateralized in the visual field when presented (1–3). Interestingly, the lateralized signature of the CDA is observed even though spatial location is not a task-relevant feature retained in memory. The CDA is observed when subjects need to remember the color (2, 4), orientation (3, 4), or shapes of objects (1, 5) for an explicit, short-term memory task. The amplitude of the CDA also appears to be sensitive to the precision or quality of the object representations that are stored (6, 7). This consistent lateralization occurs even when the information stored in memory needs to be compared with objects that can appear anywhere in the visual field (8–13), making it a particularly useful neural index in the present study.

Anterior P1 as an index of long-term memory. Previous ERP research has reported an electrophysiological signature of long-term memory. In the long-term memory ERP literature using recognition tasks and visual memoranda (14–16), changes in an early frontal positivity called the anterior P1 or P170 have been shown to be strongly predictive of the magnitude of a subject's behavioral priming effects across long retention intervals (16). A more negative anterior P1 tracks stimulus familiarity (17).

The hypothesized link between the anterior P1 and long-term memory also comes from work showing that similar potentials at approximately the same latency and elicited under similar conditions provide a measurement of the emergence of information about a prior occurrence of a stimulus that contributes to recognition judgments (18–21). Important for our present purposes, the anterior P1 is dissociable from the posterior N1 (i.e., N170) that shows short-term adaptation effects (16). Although the linkage between the anterior P1 and long-term memory has been convincingly established, the precise cognitive and biophysical mechanisms that generate the P1 remain an open topic of investigation.

Methods.

Subjects. Fifty-four subjects [experiment 1: $n = 18$, five women, mean age ± SD = 21.9 ± 3.4; experiment 2, $n = 18$, six women, mean age (years) ± SD = 21.2 ± 3.4; experiment 3, $n = 18$, five women, mean age (years) ± SD = 23.2 ± 4.9] with normal color vision and normal or corrected-to-normal visual acuity gave their informed written consent to participate in the study approved by the Vanderbilt University Institutional Review Board.

Stimuli. After anodal or sham tDCS, subjects performed a visual search task in which the target was cued on each trial (Figs. 1*B* and 2*A*). Stimuli were viewed from 114 cm on a gray background (54.3 cd/m^2). A black fixation cross (<0.01 cd/m^2, 0.4° × 0.4° of visual angle) was visible throughout each trial. Cue stimuli were presented 2.2° to the left or right of the center of the monitor, and search stimuli were arranged similar to the number of locations on a clock face, 4.4° from the center of the monitor. In experiments 1 and 3, the cue array contained one red ($x = 0.612$, $y = 0.333$, 15.1 cd/m^2) and one green ($x = 0.281$, $y = 0.593$, 45.3 cd/m^2) and the search array contained one red, one green, and 10 black distractor (<0.01 cd/m^2) Landolt-C stimuli (0.88° diameter, 0.13° thick, and 0.22° gap width) of eight possible orientations (0°, 22.5°, 45°, 67.5°, 90°, 112.5°, 135°, 157.5°). In experiment 2, the elements in the cue and search arrays were pictures of real-world objects (subtending 1.75 × 1.75 of visual angle) drawn from >2,600 categorically distinct images (22). The cue array contained one "dog" category image (out of eight possible images) and one "bird" category image (out of eight possible images), outlined in a red ($x = 0.612, y = 0.333$, 15.1 cd/m^2) or green ($x = 0.281$, $y = 0.593$, 45.3 cd/m^2; 0.13° thick, 2° diameter) circle to mark the task-relevant, real-world image with a unique color, and allow the cue stimuli to be free from physical stimulus confounds. The search array contained one dog category image and one bird category image, outlined in a red or green circle, and 10 inanimate black and white distractor images (out of eight possible images) outlined in black circles (<0.01 cd/m^2). These circles made it so that search could be completed within 2,000 ms, without excessive saccadic eye movements, and the N2pc to the target image could be measured unambiguously. The target shape (experiments 1 and 3) and circle outlining the real-world target object (experiment 2) could only appear in the task-relevant color. The task-relevant color in experiments 1 and 3 (i.e., red or green) and the task-relevant real-world object category in experiment 2 (i.e., dog or bird) of the cue stimulus were determined before the start of each experiment, counterbalanced across subjects to rule out physical stimulus confounds (23).

Trial and intertrial structure. Each trial began with fixation (1,200–1,600 ms). Next, two cue stimuli were presented for 100 ms, followed by a 1,000-ms interval during which we measured the CDA and anterior P1. The search array was then presented for 2,000 ms. The intertrial interval was 1,200–1,600 ms, randomly jittered with a rectangular distribution. In all experiments, a target was presented in half of the search arrays and matched the shape (experiments 1 and 3) or picture (experiment 2) of the task-relevant cue. Every search array contained an item that matched the color of the cue object (i.e., the possible target), but on target absent trials, this object had a different shape. Subjects responded as quickly and accurately as possible to the search array by pressing one button on a handheld gamepad (Logitech Precision) with their right hand for target present and a different button with their right hand for target absent.

Target presence (present or absent) and the target location, when present, were randomly selected on each trial. The same target was cued across a run of three, five, or seven trials randomly varying in length, with the identity of the target randomly selected for each run and without repetition in adjacent runs. Each subject completed 720 trials in each condition (sham and anodal).

tDCS. We used tDCS because it represents an effective, noninvasive technique for directly manipulating cortical brain activity by passing a weak electrical current through electrodes placed on the scalp. The tDCS was administered using a battery-driven,

constant-current stimulator (Mind Alive, Inc.) and pair of conductive rubber electrodes (active, 19.25 cm^2; reference, 52 cm^2). The electrodes were placed in saline-soaked synthetic sponges and held in place by a headband. The reference (or cathodal) electrode was placed on the center of the right cheek to avoid any confounding effects from other brain regions (24–27). Specifically, the cheek electrode was placed diagonally, 3 cm from the cheilion (lip corner at rest), along an imaginary line connecting the cheilion to the ipsilateral condylion (palpable when the jaw is moved) (Fig. 1*A*).

Current at the anodal electrode was applied for 20 min at an intensity of 2.0 mA over the medial-frontal region (site FCz, from the International 10–20 System) for experiments 1 and 2, and over the right parietal region (site P2) for experiment 3. Stimulation protocols similar to the one we used here have produced effects on behavior and electrophysiology lasting up to 4.8 h (24). These enduring effects are believed to reflect the induction of cortical plasticity from anodal stimulation having depolarized the resting state cell membrane potentials, leading to increased neuronal excitability (28). A sham tDCS condition was administered following an identical procedure, but stimulation only lasted 30 s, ramping up and down at the beginning, middle, and end of the 20-min period to simulate the periodic tingling sensation often endorsed by subjects on active testing days. Debriefing questions confirmed that subjects were blinded to the presence of stimulation.

Electrophysiological recordings. The EEG was acquired (250-Hz sampling rate, 0.01- to 100-Hz bandpass filter) using an SA Instrumentation Amplifier from 21 tin electrodes, including three midline sites (Fz, Cz, Pz), seven lateral pairs (F3/4, C3/4, P3/4, PO3/4, T3/4, T5/6, O1/2), one left occipital site (OL, halfway between O1 and T5), and one right occipital site (OR, halfway between O2 and T6), arrayed based on the International 10–20 System and embedded in an elastic cap (Electrocap International). The right mastoid electrode served as the online reference, and signals were rereferenced offline to the average of the left and right mastoids (29). The electrooculogram (EOG) was recorded using bipolar electrodes placed 1 cm lateral to the external canthi to measure horizontal eye movements and bipolar electrodes above and beneath the left eye to measure vertical eye movements and blinks. Trials containing incorrect behavioral responses or ocular or myogenic artifacts were excluded. A two-step ocular artifact rejection method was implemented (30), resulting in the removal of one subject from experiment 1 and two subjects from experiment 3 for excessive eye movements [either >25% of individual trials rejected or any residual systematic eye movement that resulted in horizontal electrooculogram (HEOG) voltage deflections >3.2 μV, corresponding to an ocular deviation of ±0.1°]. Figs. S1–S3 illustrate the HEOG waveforms time-locked to cue and search array targets for left and right visual hemifields, for each stimulation condition, and for each experiment. Grand average waveforms were 35-Hz low-pass-filtered for presentation purposes.

Data analysis. To understand the locus of the effects following our causal manipulation of the brain, we examined six distinct ERP components, each providing a neural measure of a different cognitive mechanism (23). The CDA was measured at lateral posterior parietal, occipital, and temporal electrode sites (PO3/4, O1/2, OL/R, and T5/6, respectively) as the difference in mean amplitude between the ipsilateral and contralateral waveforms during 300–1,000 ms after target cue onset (2–4, 9–11, 13). The N2pc was measured at lateral occipital electrodes (OL/R) as the mean difference in amplitude between the ipsilateral and contralateral waveforms with respect to the color of the search target during 200–300 ms following the onset of the search array (31). The anterior P1 amplitude was measured at the frontocentral electrode site (Fz) during 170–300 ms following target cue onset (11, 13, 16). We used a liberal measurement window to capture the entirety of this anterior P1 effect across all subjects but confirmed that all of the findings reported are also significant using the more conservative measurement window of 170–200 ms after cue onset (all $P < 0.05$). The posterior P1 and N1 were measured from lateral occipital electrodes (OL/R) from 75–100 ms and 125–175 ms, respectively, after search array onset, quantified as mean amplitude (32). The lateralized readiness potential (LRP) was measured from central lateral electrodes (C3/4) during the time window from −200 to 0 ms relative to correct response onset as contralateral minus ipsilateral waveforms with respect to the right hand used for the button-press responses (33). The LRP amplitude was defined as the mean amplitude in the window from LRP onset until response, and the LRP onset latency was defined as the time point at which the voltage reached 50% of the peak amplitude (34). All ERP components were baseline-corrected 200 to 0 ms before the relevant stimulus-locking event, except for the LRP, which was corrected 800–600 ms before response (33).

We computed ANOVAs using the within-subjects factors of stimulation condition (anodal vs. sham), target repetition (one vs. two to four vs. five to seven), and target color laterality (contralateral vs. ipsilateral) on RT and the amplitudes of the anterior P1, CDA, N2pc, posterior P1, N1, and LRP. Binning repetition trials increased statistical power across same-target runs, allowing us to obtain robust measures of the components of interest, consistent with prior work (11, 13, 16). Preplanned single degree of freedom contrasts were performed on the first two serial positions in a run of same-target trials to assess the speed of attentional tuning after a single instance of using a target for search. To correct for multiple comparisons, we used Fisher's least significant difference tests. *P* values were adjusted using the Greenhouse–Geisser epsilon correction for nonsphericity when this assumption was violated (35).

Current-flow model. To increase our precision in reasoning about the effects of tDCS in the brain, we computed a computational forward model of tDCS current flow. Our model of tDCS current flow was informed by previously established methods (36–39). This procedure involved (*i*) MRI segmentation, (*ii*) electrode placement, (*iii*) generation of a finite element model, and (*iv*) computation. We used the Montreal Neurological Institute T1-weighted MRI reference brain from CURRY 6.0 multimodal neuroimaging software (Compumedics Neuroscan). A combination of automated and manual segmentation tools was used to obtain tissue masks, including Gaussian filters, and morphological and Boolean operations implemented in MATLAB (MathWorks). Unlike previous models using simple geometries (e.g., spheres), we exploited realistic volumetric head geometries with a numerical solver finite element method, because this procedure should capture realistic sulci and gyri anatomy of the cortical surface, improving the precision of our tDCS model. Volumetric mesh was generated from the segmented data (>140,000 vertices, >800,000 tetrahedral elements). Segmented compartments and their respective isotropic electrical conductivities included skin (0.33 S/m), skull (0.0042 S/m), and brain (0.33 S/m). In short, the production of meshes is a process wherein each mask is divided into small contiguous elements, which then allow the current flow to be numerically computed.

Our forward computation using a finite element model was implemented in SCIRun (available as open source software at software.sci.utah.edu). We simulated current flow with a bipolar electrode configuration, including the anode (19.25 cm^2) centered over FCz (experiments 1 and 2) or P2 (experiment 3) and the cathode (52 cm^2) centered over the right cheek between the zygomaticus major and condylion. Current density corresponding to 2.0 mA of total current was applied at the anodal electrode, and the ground was applied at the cathodal electrode.

To determine the distribution of electrical potential inside the human tissues, the Laplace equation,

$$\vec{\nabla} \cdot \left(\sigma \vec{\nabla} \varphi\right) = 0$$

(φ, potential; σ, conductivity) was solved, and the following boundary conditions were used. Inward current flow = J_n (normal current density) was applied to the exposed surface of the anode. The ground was applied to the exposed surface of the cathode. All other external surfaces were treated as insulated. Plots showing the path of electrical field magnitude through brain tissue were generated in MATLAB. We chose to illustrate the solutions in units of electric field (V/m) because the electric field in the brain is directly related to neuronal activation, and for varied resistivity, the electric field, unlike current density, provides sufficient information to predict activation. Lastly, although the steps in tDCS modeling are the same, differences in protocols across publications can result in meaningful differences in current flow solutions. Thus, it is important to stress that our tDCS model serves only as a working hypothesis for where the trajectory of the electrical field passes through the brain, given our specific tDCS montages.

SI Results

Experiment 1. In the sham or baseline condition of experiment 1, we observed evidence that attention became gradually tuned to the target object across the same-target runs of trials. As RTs became faster and N2pc amplitudes increased (Fig. S1*A*), CDA amplitudes systematically decreased ($F_{2,34} = 9.274$, $P = 0.001$) (Fig. 1*G* and Fig. S1*B*) and anterior P1 amplitudes systematically increased ($F_{2,34} = 8.330$, $P = 0.006$) (Fig. 1*F*) over trials in which subjects searched for the same target. Accuracy was at a mean of 96.6% correct across all trials types and did not differ across stimulation conditions or same-target runs ($P > 0.40$). These findings conform to theories of learning and automaticity (40), which propose that as task performance gradually improves, we rely less on working memory and increasingly on long-term memory representations to fine-tune the processing of task-relevant information. Although these findings provide some support for the hypothesis that long-term memory representations play a role in controlling selection as the tuning of attention unfolds naturally, the key test of the working memory and long-term memory hypotheses of attentional control is in how they account for the rapid, one-trial improvements observed following tDCS.

In experiment 1, we show that this gradual tuning of perceptual attention to simple objects can be enhanced after 20 min of brain stimulation over the medial-frontal region. We found that this enhancement in attentional control was caused by a selective influence on the hypothesized electrophysiological index of long-term memory (i.e., the anterior P1; Fig. 1*F*), although leaving the electrophysiological index of working memory unchanged (Fig. 1*G* and Fig. S1*B*). To test further the specificity of the medial-frontal brain stimulation in experiment 1 to affect only long-term memory-driven attentional tuning, we examined other electrophysiological components known to index other cognitive mechanisms, including those cognitive mechanisms associated with low-level perceptual processing and late-stage response selection. We found that medial-frontal tDCS did not have a significant effect on these ERP components, strengthening the interpretation that the improvements in attentional tuning that we observed following brain stimulation were due to the specific manipulation of information in long-term recognition memory.

Fig. S1 *C* and *D* shows the ERP components from experiment 1 related to early perceptual processing (i.e., the posterior P1 and N1) elicited by the search array and the ERP component related to response selection (i.e., the LRP) preceding correct behavioral responses. There were no main effects of stimulation condition or target repetition and no interaction between stimulation condition and target repetition on the amplitudes of the posterior P1, N1, or LRP (statistical results are provided in Table S1). Thus, changes in early perceptual and late response-stage processes could not account for the enhanced attentional control we observed following medial-frontal stimulation.

The effects of anodal stimulation reported in the present study were measured relative to the baseline sham condition in the same subjects. The within-subjects experimental design is considered one of the strongest approaches in brain stimulation research. However, to confirm our results, we also calculated between-subjects statistical tests. Specifically, we compared data from subjects who received anodal medial-frontal stimulation (i.e., experiment 1, anodal condition) against the data from a separate group of subjects who received sham posterior parietal stimulation (i.e., experiment 3, sham condition). We found that all of the behavioral and electrophysiological results from these between-subjects analyses replicated those behavioral and electrophysiological results obtained from our within-subjects analyses reported in the main text. These results included the single-trial enhancements in anterior P1 negativity ($F_{1,17} = 4.325$, $P = 0.050$), N2pc amplitude ($F_{1,17} = 5.190$, $P = 0.036$), and RT speed ($F_{1,17} = 7.742$, $P = 0.013$), as well as the null findings of CDA amplitude ($F_{1,17} = 0.164$, $P = 0.690$) following anodal medial-frontal stimulation relative to sham.

Experiment 2. Next, we asked whether our causal manipulation of long-term, memory-driven attentional tuning would generalize beyond simple geometrical shapes to more complex objects. We designed experiment 2 to be identical to experiment 1, with the exception that Landolt-C stimuli were replaced with photographs of complex, real-world objects (Fig. 2*A*), and a new group of subjects was sampled (order of anodal and sham conditions was counterbalanced, $n = 18$).

In experiment 2, we found that medial-frontal stimulation again caused selective enhancements in only the long-term memory activity elicited by the target cues, explaining the rapid improvement in the amplitude of the N2pc component elicited by the targets and the search RTs that followed (Fig. 2 *B–E*). Relative to sham, the anodal stimulation accelerated RTs ($F_{2,34} = 4.232$, $P = 0.038$) and rapidly increased N2pc amplitude ($F_{2,34} = 4.168$, $P = 0.038$) and anterior P1 amplitudes ($F_{2,34} = 4.106$, $P = 0.048$), but had no affect on the CDA ($F_{2,34} = 0.245$, $P = 0.758$), which continued to decline in amplitude over same-target trials ($F_{2,34} = 6.695$, $P = 0.005$), but at a rate that did not differ from the sham baseline ($F_{1,17} = 0.088$ $P = 0.770$) (N2pc and CDA waveforms are provided in Fig. S2 *A* and *B*). Pairwise comparisons showed that the sharpest increase in attentional tuning for these real-world objects was between the first two trials, as shown in search RT behavior ($F_{1,17} = 9.256$ $P = 0.007$), N2pc amplitude ($F_{1,17} = 4.237$, $P = 0.050$), and anterior P1 amplitude ($F_{1,17} = 10.540$ $P = 0.005$). Accuracy was at a mean of 97.4% correct across all trials types and did not differ across stimulation conditions or same-target runs ($P > 0.35$).

As in experiment 1, we found that the rate of tDCS-mediated anterior P1 amplitude predicted the speed of an individual's improvement in search behavior after anodal stimulation ($r_{18} = 0.489$, $P = 0.039$) (Fig. 2*F*). As in experiment 1, the medial-frontal effects were selective in that electrophysiological indices of low-level perceptual processing and late-stage response selection were not affected by stimulation (Fig. S2 *C* and *D* and Table S1). These results demonstrate that our findings can be replicated and extended to conditions in which subjects search for real-world objects. Like experiment 1, our findings from experiment 2 were consistent with the view that long-term memory representations can explain rapid changes in attentional tuning, not just the working memory representations that have been the focus of the dominant theories. Finally, one alternative explanation of the anterior P1 results is that this early frontal positivity is not as deeply linked to long-term memory processes as

previously believed. The anterior P1's causal relationship with attentional improvements in the present study, combined with previous research linking this component to long-term memory, suggests that anterior P1 might play a role in the focusing of attention that activates representations maintained in long-term memory (41). Future investigations using causal techniques, such as tDCS, will be necessary to test such rival hypotheses and determine better the functional connection between the anterior P1 and mechanisms of selection guidance.

Across-Session Analyses of Experiments 1 and 2. When we aggregated data across experiments 1 and 2, we found that search RT and the anterior P1 were systematically modulated by the cumulative effects of learning across the full experimental session. An ANOVA with the factor of epoch (first third vs. second third vs. final third) revealed that RTs at the first target repetition in the runs of same-target trials became increasingly faster as subjects gained more experience on the task ($F_{2,34} = 4.366$, $P = 0.038$). Similarly, the anterior P1 amplitude grew progressively more negative over the course of the experiments ($F_{2,34} = 6.241$, $P = 0.019$). The fact that the anterior P1 responded to cumulative learning effects in this manner is consistent with current functional interpretations of this component as reflecting processes related to long-term memory. In contrast to these changes in anterior P1 and search RT, the accumulation of experience in these tasks did not systematically influence the amplitude of the CDA ($F_{2,34} = 0.713$, $P = 0.455$). The results from this learning analysis conducted across the entire experimental session, and the results we obtained from the relatively short bursts of learning measured across the same-target runs of trials, converge on the conclusion that medial-frontal stimulation changed visual search performance by influencing the nature of attentional guidance by long-term memory.

Experiment 3. In the main text, the results from experiment 3 provide evidence for the causal manipulation of perceptual processing via electrical stimulation over the parietal region. Our combined results across experiments 1–3 show that parietal stimulation affected perceptual processing and medial-frontal stimulation affected top-down attentional control by long-term memory. Here, we show additional plots of the waveforms and analyses to flesh out our findings from experiment 3 more fully.

Fig. S3*A* shows the posterior P1 and N1 waveforms across target repetition sorted by stimulation condition (i.e., either anodal or sham) and by the location of the search target color (i.e., either in the left or right visual hemifield). These N1 components are identical to the N1 shown in Fig. 4*F*, but we show the waveforms for each target repetition here (statistical results are provided in the main text and Table S1). Note that unlike the N1 component, the posterior P1 amplitude showed no significant stimulation condition × target color laterality interaction ($F_{1,17} = 0.104$, $P = 0.751$) and no main effects of stimulation condition ($F_{1,17} = 0.004$, $P = 0.951$) or target color laterality ($F_{1,17} = 0.400$, $P = 0.536$), indicating that our parietal tDCS configuration had a selective influence on the N1 component related to the early perceptual processing of the visual search stimuli.

Fig. S3 *B* and *C* shows the CDA and N2pc waveforms from experiment 3 sorted by stimulation condition and the location of the cue or search target in the visual field, respectively. Neither of these components was significantly changed by target laterality (N2pc $F_{1,17} = 0.025$, $P = 0.876$; CDA $F_{1,17} = 0.356$, $P = 0.559$) or stimulation condition (N2pc: $F_{1,17} = 0.031$, $P = 0.862$; CDA $F_{1,17} = 1.916$, $P = 0.184$) (additional statistical results are provided in the main text). Similarly, the anterior P1 was not affected by target laterality ($F_{1,17} = 0.210$, $P = 0.653$) or stimulation condition ($F_{1,17} = 0.126$, $P = 0.727$) (additional statistical results are provided in the main text) (Fig. S3*D*). Accuracy was at a mean of 98.2% correct across all trial types and did not differ across stimulation conditions or same-target runs ($P > 0.35$). These results indicate our parietal stimulation protocol had no measurable influence on the cognitive mechanisms of covert attentional selection (indexed by the N2pc), working memory (indexed by the CDA), or long-term memory (indexed by the anterior P1). Thus, changes in the early perceptual processing of the search stimuli (indexed by the posterior N1) were the source of the bidirectional effects we observed in search behavior following parietal tDCS.

As reported in the main text, the processes of input selection and attentional guidance did exhibit their characteristic modulations across same-target trials in experiment 3, indicating their role in the tuning of attention that unfolds across trials of searching for the same object (40). Specifically, the waveforms in Figs. S3*D* and S4 show a steady increase in the negativity of the anterior P1, decline in CDA amplitude, and increase in N2pc amplitude as subjects searched for the same target (statistical results are provided in the main text). Thus, despite the influence of parietal stimulation on subjects' perceptual processing of the search arrays, the deployment of attention and the memory representations providing top-down control of attention continued to function in a normal fashion, unchanged by the improvements and impairments we observed in perceptual processing and behavior following parietal tDCS.

As in experiments 1 and 2, we examined the ERP component known to index motor preparation activity and response-stage processing (i.e., the LRP). Fig. S3*E* shows the LRP waveforms for each target repetition and stimulation condition from experiment 3. No significant results were found (Table S1). This again underscores the conclusion that parietal stimulation had a selective impact on perceptual processing, in contrast to the effects of medial-frontal tDCS on the long-term memory representations providing top-down attentional control.

tDCS Modeling Results. To visualize the brain areas affected by our tDCS manipulations, we computed a forward computational model of the current flow. Fig. 1*A* shows the pattern of current flow during anodal medial-frontal tDCS based on our stimulation protocol and standard estimates of underlying anatomy and tissue properties. Electrical fields were modeled as extending through the dorsal subdivision of the medial-frontal cortex, including such areas as the anterior cingulate cortex, supplementary motor area (SMA), and presupplementary motor area (pre-SMA). A higher intensity of current is likely to have influenced more dorsal or superficial areas of cortex, such as the SMA and pre-SMA. Due to the position of the cathodal electrode placed over the right cheek in our stimulation montage, the right dorsolateral cortex also appeared to be implicated to a lesser extent. Moreover, because of the highly interconnected nature of frontal cortex, we cannot rule out the possibility that tDCS induced neural activity in distally connected brain areas outside the regions of activation predicted by our model. Follow-up studies using neuroimaging techniques are needed to identify definitively the brain areas and associated networks responsible for the rapid changes in perceptual attention we observed following medial-frontal stimulation. However, in this study, we rely on the qualitative predictions our modeling solution provides about the likely spatial distribution of the electrical field through the brain.

Fig. 4*A* shows the model prediction of the current-flow pattern during tDCS using the P2 electrode position as the anodal site of stimulation paired with the cathodal electrode over the right cheek. The gravity center of the electrical field was situated in the right hemisphere of the superior parietal lobule (Brodmann's areas 5 and 7). However, right lateralized extrastriate visual areas, such as the superior occipital gyrus (Brodmann's area 19),

also appeared to have been in the path of current flow. Future work will be necessary to determine the brain areas affected by this montage more precisely and the possibility of remote activations not captured by tDCS models.

1. Ikkai A, McCollough AW, Vogel EK (2010) Contralateral delay activity provides a neural measure of the number of representations in visual working memory. *J Neurophysiol* 103(4):1963–1968.
2. Vogel EK, Machizawa MG (2004) Neural activity predicts individual differences in visual working memory capacity. *Nature* 428(6984):748–751.
3. Vogel EK, McCollough AW, Machizawa MG (2005) Neural measures reveal individual differences in controlling access to working memory. *Nature* 438(7067):500–503.
4. Woodman GF, Vogel EK (2008) Selective storage and maintenance of an object's features in visual working memory. *Psychon Bull Rev* 15(1):223–229.
5. Luria R, Sessa P, Gotler A, Jolicoeur P, Dell'Acqua R (2010) Visual short-term memory capacity for simple and complex objects. *J Cogn Neurosci* 22(3):496–512.
6. Machizawa MG, Goh CC, Driver J (2012) Human visual short-term memory precision can be varied at will when the number of retained items is low. *Psychol Sci* 23(6): 554–559.
7. Anderson DE, Vogel EK, Awh E (2011) Precision in visual working memory reaches a stable plateau when individual item limits are exceeded. *J Neurosci* 31(3):1128–1138.
8. Woodman GF, Arita JT (2011) Direct electrophysiological measurement of attentional templates in visual working memory. *Psychol Sci* 22(2):212–215.
9. Carlisle NB, Arita JT, Pardo D, Woodman GF (2011) Attentional templates in visual working memory. *J Neurosci* 31(25):9315–9322.
10. Reinhart RMG, Carlisle NB, Woodman GF (2014) Visual working memory gives up attentional control early in learning: Ruling out interhemispheric cancellation. *Psychophysiology* 51(8):800–804.
11. Woodman GF, Carlisle NB, Reinhart RMG (2013) Where do we store the memory representations that guide attention? *J Vis* 13(3):1–7.
12. Gunseli E, Olivers CNL, Meeter M (2014) Effects of search difficulty on the selection, maintenance, and learning of attentional templates. *J Cogn Neurosci* 26(9):2042–2054.
13. Reinhart RMG, Woodman GF (2014) High stakes trigger the use of multiple memories to enhance the control of attention. *Cereb Cortex* 24(8):2022–2035.
14. Danker JF, et al. (2008) Characterizing the ERP Old-New effect in a short-term memory task. *Psychophysiology* 45(5):784–793.
15. Paller KA, Lucas HD, Voss JL (2012) Assuming too much from 'familiar' brain potentials. *Trends Cogn Sci* 16(6):313–315, discussion 315–316.
16. Voss JL, Schendan HE, Paller KA (2010) Finding meaning in novel geometric shapes influences electrophysiological correlates of repetition and dissociates perceptual and conceptual priming. *Neuroimage* 49(3):2879–2889.
17. Hamann SB, Squire LR (1997) Intact perceptual memory in the absence of conscious memory. *Behav Neurosci* 111(4):850–854.
18. Tsivilis D, Otten LJ, Rugg MD (2001) Context effects on the neural correlates of recognition memory: An electrophysiological study. *Neuron* 31(3):497–505.
19. Duarte A, Ranganath C, Winward L, Hayward D, Knight RT (2004) Dissociable neural correlates for familiarity and recollection during the encoding and retrieval of pictures. *Brain Res Cogn Brain Res* 18(3):255–272.
20. Friedman D (2007) ERP studies of recognition memory: Differential effects of familiarity, recollection, and episodic priming. *New Research in Cognitive Sciences*, ed Sun M-K (Nova Science Publishers, Inc., Hauppauge, NY), Vol 1, pp 63–93.
21. Diana RA, Vilberg KL, Reder LM (2005) Identifying the ERP correlate of a recognition memory search attempt. *Brain Res Cogn Brain Res* 24(3):674–684.
22. Brady TF, Konkle T, Alvarez GA, Oliva A (2008) Visual long-term memory has a massive storage capacity for object details. *Proc Natl Acad Sci USA* 105(38):14325–14329.
23. Woodman GF (2010) A brief introduction to the use of event-related potentials in studies of perception and attention. *Atten Percept Psychophys* 72(8):2031–2046.
24. Reinhart RMG, Woodman GF (2014) Causal control of medial-frontal cortex governs electrophysiological and behavioral indices of performance monitoring and learning. *J Neurosci* 34(12):4214–4227.
25. Berryhill ME, Wencil EB, Branch Coslett H, Olson IR (2010) A selective working memory impairment after transcranial direct current stimulation to the right parietal lobe. *Neurosci Lett* 479(3):312–316.
26. Hsu TY, et al. (2011) Modulating inhibitory control with direct current stimulation of the superior medial frontal cortex. *Neuroimage* 56(4):2249–2257.
27. Tseng P, et al. (2012) Unleashing potential: Transcranial direct current stimulation over the right posterior parietal cortex improves change detection in low-performing individuals. *J Neurosci* 32(31):10554–10561.
28. Nitsche MA, et al. (2008) Transcranial direct current stimulation: State of the art 2008. *Brain Stimulat* 1(3):206–223.
29. Nunez PL (1981) *Electric Fields of the Brain* (Oxford Univ Press, New York).
30. Woodman GF, Luck SJ (2003) Serial deployment of attention during visual search. *J Exp Psychol Hum Percept Perform* 29(1):121–138.
31. Woodman GF, Luck SJ (1999) Electrophysiological measurement of rapid shifts of attention during visual search. *Nature* 400(6747):867–869.
32. Luck SJ, Hillyard SA (1990) Electrophysiological evidence for parallel and serial processing during visual search. *Percept Psychophys* 48(6):603–617.
33. Smulders FTY, Miller JO (2012) The lateralized readiness potential. *Oxford Handbook of Event-Related Potential Components*, eds Luck SJ, Kappenman E (Oxford Univ Press, New York), pp 209–229.
34. Miller J, Patterson T, Ulrich R (1998) Jackknife-based method for measuring LRP onset latency differences. *Psychophysiology* 35(1):99–115.
35. Jennings JR, Wood CC (1976) Letter: The epsilon-adjustment procedure for repeated-measures analyses of variance. *Psychophysiology* 13(3):277–278.
36. Wagner T, et al. (2007) Transcranial direct current stimulation: A computer-based human model study. *Neuroimage* 35(3):1113–1124.
37. De Lucia M, Parker GJ, Embleton K, Newton JM, Walsh V (2007) Diffusion tensor MRI-based estimation of the influence of brain tissue anisotropy on the effects of transcranial magnetic stimulation. *Neuroimage* 36(4):1159–1170.
38. Sadleir RJ, Vannorsdall TD, Schretlen DJ, Gordon B (2010) Transcranial direct current stimulation (tDCS) in a realistic head model. *Neuroimage* 51(4):1310–1318.
39. Bikson M, Rahman A, Datta A (2012) Computational models of transcranial direct current stimulation. *Clin EEG Neurosci* 43(3):176–183.
40. Logan GD (2002) An instance theory of attention and memory. *Psychol Rev* 109(2): 376–400.
41. Cowan N (1997) *Attention and Memory* (Oxford Univ Press, New York).

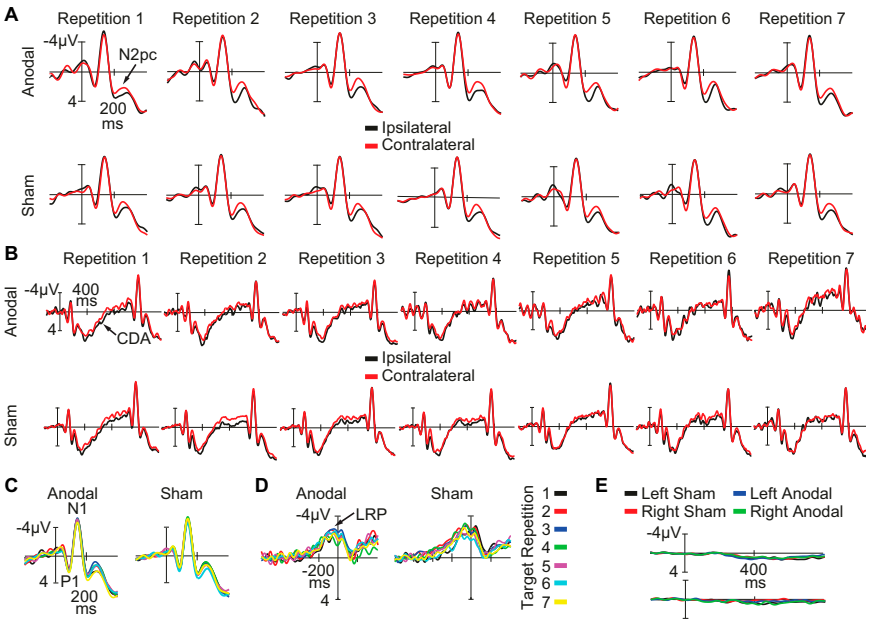

Fig. S1. Sensory, response, attention, and working memory ERPs from experiment 1. (*A*) Search array-locked grand average potentials at lateral occipital sites (OL/OR) contralateral (red) and ipsilateral (black) to the location of the target color shown across repetitions 1–7 from anodal and sham tDCS conditions. (*B*) Cue-locked grand average potentials at lateral occipital sites (OL/OR) contralateral (red) and ipsilateral (black) to the location of the target shown across repetitions 1–7 from anodal and sham tDCS conditions. (*C*) Search array-locked grand average potentials at lateral occipital sites (OL/OR) contralateral with respect to target color location shown across target repetitions 1–7 from anodal and sham tDCS conditions. (*D*) Response-locked grand average difference waves (contralateral minus ipsilateral with respect to response hand) at central lateral sites (C3/C4) from correct trials shown across target repetitions 1–7 from anodal and sham tDCS conditions. (*E*) Cue-locked (*Top*) and search array-locked (*Bottom*) HEOG waveforms for targets in the left and right visual hemifields and across tDCS conditions. Labels show the posterior P1, N1, LRP, N2pc, and CDA.

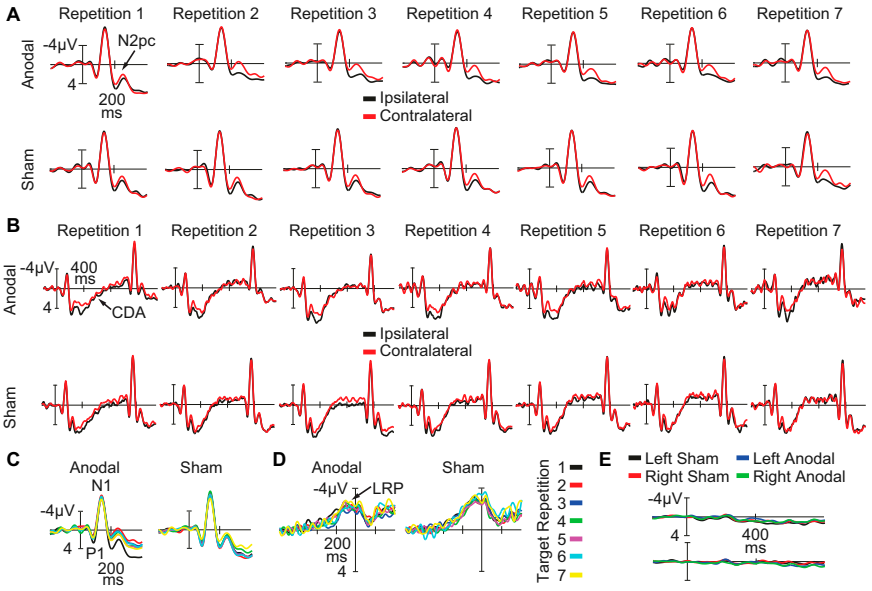

Fig. S2. Sensory, response, attention, and working memory ERPs from experiment 2. (*A*) Search array-locked grand average potentials at lateral occipital sites (OL/OR) contralateral (red) and ipsilateral (black) to the location of the target color shown across repetitions 1–7 from anodal and sham tDCS conditions. (*B*) Cue-locked grand average potentials at lateral occipital sites (OL/OR) contralateral (red) and ipsilateral (black) to the location of the target shown across repetitions 1–7 from anodal and sham tDCS conditions. (*C*) Search array-locked grand average potentials at lateral occipital sites (OL/OR) contralateral with respect to target color location shown across target repetitions 1–7 from anodal and sham tDCS conditions. (*D*) Response-locked grand average difference waves (contralateral minus ipsilateral with respect to response hand) at central lateral sites (C3/C4) from correct trials shown across target repetitions 1–7 from anodal and sham tDCS conditions. (*E*) Cue-locked (*Top*) and search array-locked (*Bottom*) HEOG waveforms for targets in the left and right visual hemifields and across tDCS conditions. Labels show the posterior P1, N1, LRP, N2pc, and CDA.

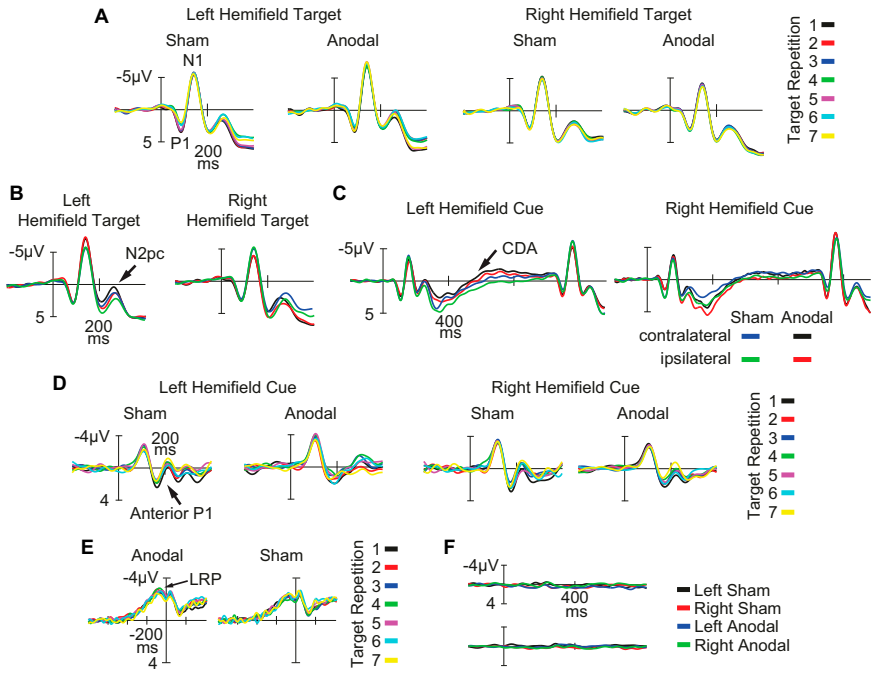

Fig. S3. Sensory, attention, working memory, long-term memory, and response ERPs from experiment 3. (*A*) Search array-locked grand average potentials at lateral occipital sites (OL/OR) contralateral to left and right hemifield target color locations shown across repetitions and tDCS conditions. (*B*) Search array-locked grand average potentials at lateral occipital sites (OL/OR) contralateral and ipsilateral with respect to left and right hemifield target color location shown for each tDCS condition and collapsed across target repetitions. (*C*) Cue-locked grand average potentials at lateral occipital sites (OL/OR) contralateral and ipsilateral to the location of the target cue shown for each tDCS condition and collapsed across target repetitions. (*D*) Cue-locked grand average potentials at the frontal midline electrode (Fz) shown across target repetitions and sorted by left and right hemifield target cue location and tDCS condition. (*E*) Response-locked grand average difference waves (contralateral minus ipsilateral with respect to response hand) at central lateral sites (C3/C4) from correct trials shown across target repetitions and tDCS conditions. (*F*) Cue-locked (*Top*) and search array-locked (*Bottom*) HEOG waveforms for targets in the left and right visual hemifields and across tDCS conditions. Labels show the posterior P1 and N1, N2pc, CDA, anterior P1, and LRP.

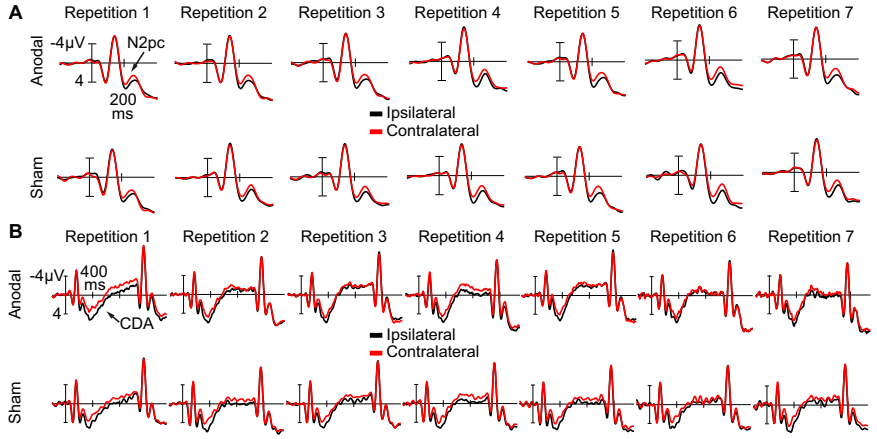

Fig. S4. Attention and working memory ERPs from experiment 3. (*A*) Search array-locked grand average potentials at lateral occipital sites (OL/OR) contralateral (red) and ipsilateral (black) to the location of the target color shown across repetitions 1–7 from anodal and sham tDCS conditions. (*B*) Cue-locked grand average potentials at lateral occipital sites (OL/OR) contralateral (red) and ipsilateral (black) to the location of the target cue shown across repetitions 1–7 from anodal and sham tDCS conditions. Labels show the N2pc and CDA.

Table S1. Summary of statistical results on the amplitude of the posterior P1, N1, and LRP from experiments 1–3

ERP components	Stimulation condition	Target repetition	Stimulation condition × target repetition
Experiment 1			
Posterior P1	$F_{1,17} = 0.795$, $P = 0.385$	$F_{2,34} = 0.619$, $P = 0.482$	$F_{2,34} = 0.021$, $P = 0.919$
N1	$F_{1,17} = 0.177$, $P = 0.679$	$F_{2,34} = 0.329$, $P = 0.589$	$F_{2,34} = 0.310$, $P = 0.597$
LRP	$F_{1,17} = 0.768$, $P = 0.393$	$F_{2,34} = 2.363$, $P = 0.116$	$F_{2,34} = 0.662$, $P = 0.458$
Experiment 2			
Posterior P1	$F_{1,17} = 2.536$, $P = 0.130$	$F_{2,34} = 0.943$, $P = 0.355$	$F_{2,34} = 1.799$, $P = 0.196$
N1	$F_{1,17} = 0.062$, $P = 0.806$	$F_{2,34} = 0.182$, $P = 0.687$	$F_{2,34} = 0.009$, $P = 0.933$
LRP	$F_{1,17} = 0.748$, $P = 0.399$	$F_{2,34} = 0.752$, $P = 0.414$	$F_{2,34} = 1.765$, $P = 0.200$
Experiment 3			
Posterior P1	$F_{1,17} = 3.988$, $P = 0.062$	$F_{2,34} = 2.138$, $P = 0.147$	$F_{2,34} = 0.293$, $P = 0.734$
N1	$F_{1,17} = 0.316$, $P = 0.582$	$F_{2,34} = 1.132$, $P = 0.305$	$F_{2,34} = 0.143$, $P = 0.773$
LRP	$F_{1,17} = 0.311$, $P = 0.585$	$F_{2,34} = 0.041$, $P = 0.930$	$F_{2,34} = 0.364$, $P = 0.643$